Magnets, Magnetism, and Magnetic Resonance Imaging: History, Basics, Clinical Aspects, and Future Directions

Shatadru Chakravarty and Erik M. Shapiro

Abstract Magnets and magnetism have played an intriguing and controversial role in human medicine. Undoubtedly, the most relevant use of magnetic phenomenon in modern clinics pertains to the diagnostic potential of Magnetic Resonance Imaging (MRI) that employs low-intensity radiofrequency electromagnetic radiation to study subjects placed in a strong magnetic field. The physical basis of MRI lies in its inherent ability to monitor the temporal and spatial distribution of tissue water protons, in the process taking into account local abnormalities to generate images with variable contrast. The contrast produced in MRI is further enhanced by the administration of paramagnetic entities called contrast agents that allow for superior spatial resolution in MRI. This chapter gives a glimpse into the history and development of MRI as a diagnostic imaging tool. The fundamentals of the MRI technique, contrast agent design, their current clinical status, and future directions are also discussed.

Keywords Magnetic resonance imaging · Contrast agents · Gadolinium · Nephrogenic systemic fibrosis

1 Introduction

Man's tryst with magnets and magnetism in general dates back to ancient times when the phenomenon of *aurora borealis* (or the northern lights) was first being observed [1]. It was, however, not until 1200 BC that an understanding of the general principles of magnetism began to develop with advances in iron smelting and the term 'magnetite' (coined to refer to iron oxide, Fe_3O_4) came into existence. The first exposition on the properties of magnetized needles was authored by Petrus Peregrinus in 1269 [2]. It was not until the year 1600 that a more enhanced and

S. Chakravarty (✉) · E. M. Shapiro
Department of Radiolgy, Michigan State University, 846 Service Road, East Lansing, MI, USA
e-mail: shatadru2006@gmail.com; shatadru@msu.edu

Institute for Quantitative Health Sciences and Engineering, Michigan State University, 775 Woodlot Dr, East Lansing, MI, USA

G. Dutta et al. (eds.), *Modern Techniques in Biosensors*, Studies in Systems, Decision and Control 327, https://doi.org/10.1007/978-981-15-9612-4_6

scientific treatise, including the discovery of earth's own magnetic properties was presented by the English physician, William Gilbert in his much-celebrated book *De Magnete* [3]. It is still widely considered to be a pioneering work in early scientific research. In medicine, magnetite or lodestone was considered to possess miraculous healing properties, stemming from the early belief that magnetite has a soul of its own, justified by its ability to move iron particles, just as the soul was believed to produce motion. The earliest proponent of this ancient theory was the Greek astronomer Thales of Miletus [4]. Magnetite's use as an effective agent to control bleeding and hemorrhage was championed by Hippocrates of Cos and his pupils [5]. In addition, there were references to using this ore for the treatment of burns, arthritis, gout, poisoning, and baldness. Together with these widespread external uses of magnetite, the Egyptian physician Avicenna (980–1037 AD) doctored its uptake with milk in order to facilitate the intestinal excretion of poisonous iron rust from the body of a patient [6]. The attracting prowess of a magnet was also put into use for surgical procedures, the earliest example being that of a Hindu surgeon Sucruta (600 BC) who employed it to remove an iron arrow tip. Other noted examples include its use as a cure for hernia and removal of iron dust or metal particles from the eye during the late sixteenth century [7]. However, most of these medical and surgical applications of lodestone were explicitly disqualified by Gilbert at the end of the sixteenth century who advocated its use only for the treatment of chlorosis [8].

Over the next 300 years, detailed practical accounts on the use of magnets for surgical procedures were being published. Most of these procedures put into use increasingly complex techniques employing either native magnets or artificial electromagnets for the removal of small iron or steel particles that had accidentally got into the eyes. The ophthalmic use of electromagnets was pioneered by two feuding compatriots, Dr. Julius Hirschberg from Germany who advocated the removal of small objects from the back of the eye, and the Swiss ophthalmologist Otto Haab, who insisted on removal from the front. Both these procedures were, however, rendered equally harmful in terms of consequent damage to the iris and related side effects. Subsequently, modern advancements in eye surgery techniques and instrumentation have rendered these techniques obsolete.

On a related note, the magnetic properties of lodestone and other artificial magnets was used as a cure for nervous disorders and moral conduct. Probably, the greatest champion of this treatment modality was Franz Anton Mesmer, a physician in Vienna who assumed that magnets worked by their ability to reorient the flow of universal 'fluidum' in a patient's body. His methods gained immense popularity, initially in Vienna and then in Paris, and were considered to be a clever mix of hypnotism and psychotherapy. Later on, several experiments conducted by Benjamin Franklin and Antoine Lavoisier conclusively indicated that *suggestibility and not magnetism* had a psychological impact on the patients who were subjected to this new treatment method and were subsequently cured because of their faith in it [9]. In modern times, magnets are still believed to have healing properties and are marketed in various size and shapes to be used as a suggested cure for headaches and even cancer [10].

2 Magnetism in Medicine

With the development of superconducting electromagnets at the Bell laboratories in 1961, followed by the evolution of strong permanent magnets [11], varying medical applications for these materials in increasingly diverse fields such as radiology, dentistry, cardiology, oncology, and neurosurgery began to appear. One of the most promising outcomes of these new techniques was the miniaturization of a magnet to an extent that it could be placed at the tip of a catheter and consequently used in recording electronic signals within the brain or treatment of arterial aneurysms [12] and related heart ailments [13]. The successful use of such catheter devices requires a strong magnetic navigation system that can guide them to the area of interest for site-specific delivery of radiation or therapeutic agents. Typically, such systems employ robust superconducting magnets [14] or more recently NdFeB [neodymium(Nd)-iron(Fe)-boron(B)] permanent magnets; used in the *Niobe*® system, developed by Stereotaxis Inc., in St. Louis, Missouri. Incidentally, this system was approved by the FDA in 2003 for multiple interventional cardiology and electro-physiology procedures.

Alternately, an external magnetic field has also been used for the localization of magnetic particles-such as nano- or micro-spheres in close vicinity to tumors or other target areas, such as blood vessels and arteries [15]. Such spheres can be encapsulated with therapeutic agents for a programmed release, triggered via irradiation at a specified frequency [16] or can act via the embolization (blockage) of vessels and capillaries or a combination of both [17]. An extension of this novel treatment modality, termed as 'Magnetic Fluid Hyperthermia' (MFH), involving the action of 'magnetite nanoparticles encapsulated in a dextran coating' on tumors was proposed by both Jordan et al. and Chang et al. in the year 1993 [18]. By 2003, Jordan had started phase II clinical trials of radiation therapy coupled with magnetic hyperthermia [19, 20] with a sample size of eight patients and achieved considerable success with minimal side effects [21].

The widespread use of magnets and magnetism in various treatment modalities is truly exceptional. However, the greatest medical boon of magnetism has been its applicability in the design of various methods for enhanced disease detection. In particular, the development of *Magnetic Resonance Imaging* or *MRI*, a Nuclear Magnetic Resonance (NMR) imaging technique as a clinical diagnostic tool has revolutionized the field of early disease diagnosis. Over the past three decades, MRI (Magnetic Resonance Imaging) has been the method of choice for in vivo imaging [22]. MRI employs low-intensity radiofrequency electromagnetic waves to study materials placed in a strong magnetic field. It is best suited for non-calcified tissue and has inherently superior contrast scale and better spatial resolution than X-Ray, Computed Tomography (CT), Single Photon Emission Computed Tomography (SPECT), or Positron Emission Tomography (PET). An inherent advantage of MRI over the other techniques is that it does not involve exposure to any harmful radiation. In some cases, MRI is the only way to do clear-cut diagnosis especially in the detection of cerebral abnormalities, multiple sclerosis, and in cases where

bone artifacts are present in CT images [23]. In addition, MRI can also be used to monitor organ function using a relatively new technique called functional MRI or *f*MRI [24]. The development of MRI has also led to the extensive use of a potentially toxic and obscure lanthanide metal, *Gadolinium* (*Gd*) as a pharmaceutical agent that once injected into a patient can magnetically caress the water protons to produce startling effects in a magnetic resonance (*MR*) image. The *contrast* so produced aids the clinicians in alienating the healthy and normal tissues from the diseased ones and to indicate the status of organ function or blood flow. The chemical species that bring about such enhancements in MR images are termed as *Contrast Agents* (*CAs*). In addition to Gadolinium, contrast agents based on iron oxide nanoparticles and a manganese, Mn(II) complex have also been approved for clinical use, however, these have met with limited success commercially. Currently, all the eight contrast agents that are approved for clinical use and available commercially in the United States are small-molecule complexes with Gadolinium as the central metal ion. These *Gadolinium-based contrast agents (GBCAs)* are used in about 40% of all MRI exams and roughly 60% of all neural MRI exams, resulting in nearly 40 million uses of GBCAs worldwide [25]. In this chapter, we will discuss the various MRI contrast agents used in the clinics with recent examples, discuss their shortcomings and finally present a future outlook. However, to begin with, an interlude on the early developments of MRI as an imaging technique, its physical principles, and the logic behind the genesis of MRI CAs has been presented.

3 MRI-A Historical Perspective

On a strictly physical basis, MRI is an extension of the science underlying the nuclear magnetic resonance technique. The general experiment involves application of a time-varying magnetic field gradient to the subject of interest, followed by a spatial and temporal encoding of the resulting signals obtained from the NMR active nuclei (e.g., protons) present therein, thus generating an image [26]. The intensity of the images so obtained is augmented or curtailed by the nuclear relaxation times that in turn can be influenced by paramagnetic agents. The obvious chemical choice for a paramagnetic entity is a transition or a lanthanide metal ion, which have unpaired electrons that can influence the relaxation times of surrounding nuclei via dipolar interactions. Most of these metal ions are however extremely toxic in their native form and therefore can only be administered as complexes with multi-dentate metal chelator ligands. Such metal-ligand complexes must be water-soluble and extremely stable, both thermodynamically and kinetically, for in vivo use. A better understanding for successful application of the MRI technique would therefore require investigations into the physical behavior of aqueous solutions of such complexes in presence of a strong magnetic field with special emphasis on enhancing the relaxation rates of water protons. The following paragraph presents a small epilogue of the preliminary efforts carried out in this direction.

Initial experiments to augment the relaxation rates of nearby water protons using ferric nitrate, a paramagnetic salt was carried out by Bloch in 1948 [27]. The much-celebrated and now firmly established Solomon-Bloembergen-Morgan (SBM) theory and its various modifications aided immensely in underlining the basic physical principles of solvent proton relaxation rates for aqueous solutions of paramagnetic entities [28–32]. In 1961, Eisinger and co-workers showed that the binding of various transition metal ions such as Cu(II), Mn(II), and Cr(III) with exterior sites, such as phosphate groups within the DNA macromolecule can lead to enhanced water proton relaxation rates [33]. For decades, however, magnetic resonance was used to determine chemical structures and it was not until 1973 that the seminal work of Paul Lauterbur [34] and later improvements introduced by Peter Mansfield, led to the idea of using it for imaging the human body [35]. It was in 1977 when the first imaging studies on humans were performed [36, 37]. Once the idea of using magnetic resonance for human imaging found a strong footing, there was an increasing curiosity towards using it to alienate between healthy and diseased tissues. The answers arrived within a year when in 1978, Lauterbur and co-workers showed that normal and infarcted myocardial tissues can be differentiated based on the longitudinal proton relaxation rates ($1/T_1$) derived from tissue samples of a dog injected with a paramagnetic Mn(II) salt [38]. The idea of using a paramagnetic agent for MR imaging further gained strength with similar experiments carried out with excised dog hearts [39]. Interestingly, such contrast was only observed in the presence of the paramagnetic Mn(II) species. With considerable success in animals, Young and co-workers performed the first contrast agent assisted imaging study in humans in 1981, using ferric chloride to diagnose the gastrointestinal tract [40].

The field of CA development was, however, truly revolutionized with the arrival of CAs with a central paramagnetic gadolinium lanthanide metal ion. The idea was first proposed by Carr and co-workers who used the Gd(III) diethylenetriamine pentaacetate; $[Gd(DTPA)(H_2O)]^{2-}$ in patients with cerebral tumors and observed lesion enhancement in the images so obtained [41]. After multiple clinical trials, $[Gd(DTPA)(H2O)]^{2-}$ was approved for clinical use in 1988 [42], thus leading to an unprecedented and extensive foray into the development of novel contrast agents with an enhanced imaging profile. The majority of CAs approved for clinical use are Gd-chelates, that contain a central paramagnetic Gd(III) ion complexed using a *linear chain* or *macrocyclic* multi-dentate ligand. As discussed beforehand, CAs based on iron oxide nanoparticles and small-molecule Mn(II) chelate have also been developed and have been either used in human clinical trials or have received approval for clinical trials. However, all such agents are either no longer available commercially or their clinical development has been discontinued and they are no longer used as contrast agents for MRI [22]. In this chapter, our focus will only be on clinically approved GBCAs that are currently available and marketed.

Ongoing research aims at the generation of new and more effective class of CAs that have an enhanced MR image profile. This search clearly requires a deep understanding of the physics behind the MRI and answering one of the most pertinent questions; "*how the contrast is produced and how to improve on it*…" The following section provides a simple treatise as to how the MRI functions and the basic principles

involved in generating the desired contrast. This section will also introduce various terms pertinent to the relaxation process that would enable a better understanding of the MR imaging phenomenon.

4 How the MRI Works

In a very general sense, MRI monitors the differential distribution of water within the subject of interest. It measures the spatial variation of *proton longitudinal* (T_1) and *transversal (T_2) magnetic relaxation times.* These terms will be explained later in the section in detail. Additionally, MRI takes advantage of the contrast produced within local sections of healthy and diseased parts of the same tissue. The proton relaxation times T_1 and T_2 are sensitive to biochemical conditions, such as pH, water concentration, and temperature. The essence of MRI is thus based on the *relaxation of tissue water protons subjected to an external magnetic field*.

Prior to understanding the functional principles of the MRI, let us look at its basic hardware components. A typical MRI scanner consists of the following parts; the magnet, gradient coils, radiofrequency transmitters, radiofrequency receivers, and finally a computer to process all the signals and produce an image for analysis by a trained radiologist. These components are shown in a schematic way in Fig. 1. The most important and expensive part of the MRI is the magnet at its core. These are mostly superconducting magnets, constructed of Niobium-Titanium alloy, though

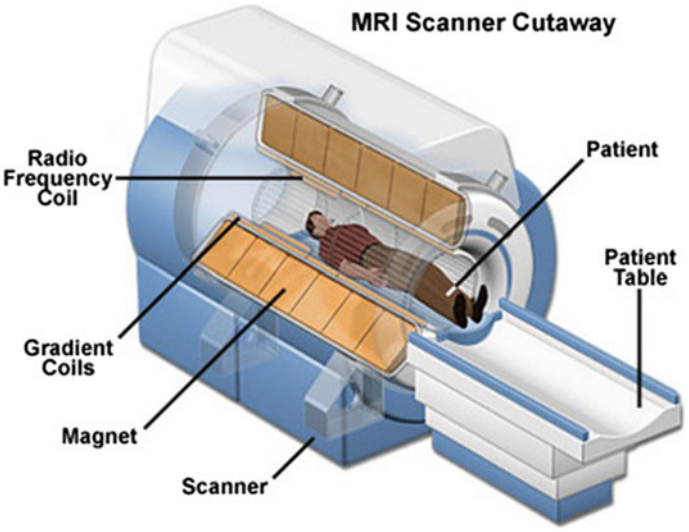

Fig. 1 A MRI scanner cutaway showing its various hardware components. Taken from Mahir Rashid & Fardin Kibria "MRI Scan-Components and Functions" https://snc2dmri.weebly.com/components--functions.html, 8 July 2020

other combination alloys such as Niobium-Tin can also be used. The strength of the MRI magnet is measured in units of Tesla (T); typical human MRI scanners range from 0.5 to 4.0 T while preclinical small animal scanners can be upto 7.0 T and 9.4 T. To establish a very stable field originating from such magnets, current flow within the superconducting coils is maintained indefinitely and the temperature is kept below the critical value by cooling them in an envelope of liquid helium. Resistive coils, also known as shim coils, and ferromagnetic blocks are housed within the magnet bore to even out field inhomogeneity. The shim coils are also used to generate fields that vary as a function of position.

The gradient coils are primarily used to produce a linear gradient in the magnetic field along one direction. Typically, the *z-axis* runs along the direction of the field and a *Maxwell coil* is used to generate a linear variation along the *z*-axis. To produce a gradient along the *x*- or *y-axes*, saddle coils, such as the *Golay coil*, are used. For producing gradients along directions other than the *x*-, *y*- or *z-axes*, currents are run along these axial coils in a proportionate manner. The gradient coils are also crucial for reducing the heat deposition and current requirements.

Another major component of the MRI system is the radiofrequency (RF) coils that are used to *transmit signals to* and *receive signals from* the subject of interest or the patient. Coils can be dual-purpose, which means that a single coil can be used to both transmit and receive signal or there can be separate, individual coils. RF coils are categorized as surface coils and volume coils. Surface coils rest on the surface of the object under consideration and can produce excellent images from the region of interest. Such images exhibit high signal-to-noise (*S*/*N*) ratio. Volume coils, on the other hand, are critical for imaging larger areas, such as the whole body or specific regions of interest such as the head or a limb. Thus, volume coils can be used to produce a homogenous field over a larger area and provide greater depth of penetration.

Finally, the entire scanning operation is controlled using a computer (not shown in Fig. 1) which also processes the signal obtained into a readout image on the MRI. For further details about specifics about each hardware component of the MRI, readers are directed towards various publications [43–45].

In order for a deeper insight into the process, let us consider a proton. A proton is a subatomic particle, which has a positive charge and a mass. What it additionally possesses is a term called "*spin*". The spin of the proton is denoted by the symbol I. As a result, the proton also has an angular momentum, characterized by its mass and charge as well as a magnetic moment, μ. What this means in a very general term is that the proton behaves as a tiny, subatomic magnet.

Now, let us consider this proton, a tiny magnet, in an external magnetic field, B_0. As the proton possesses a spin and has a charge, it undergoes a motion similar to that of a spinning top. This *precessional* motion of a proton under the influence of a field B_0 is characterized by a frequency, ν called the *Larmor frequency* and is defined by the relation; $\nu = \gamma B_0$; where γ is called the *gyromagnetic ratio* of the proton. For a proton, the value of the spin I is 1/2 and this means that in an external magnetic field (B_0) it can have a total of *two* ($2I + 1$; $I = 1/2$) possible orientations; one being aligned and the other being opposite to the direction of B_0. The alignment in the

direction of B_0 is energetically more favorable and as a result, there is an excess population of protons, and consequently an excess number of nuclear spins, aligned with the external field. This introduces a net magnetization along the external field, termed as the *longitudinal* magnetization, M_0. However, the random distribution of spins ensures that there is *no transverse* magnetization, or in simpler terms, there is no net magnetization along the plane perpendicular to the direction of B_0.

Now, the net longitudinal magnetization, M_0 has a spin of its own. As a result, a small additional magnetic field, B_1 applied perpendicular or transverse to M_0, tends to rotate M_0 towards itself. The degree to which B_1 can rotate M_0 towards itself is dependent on its strength. This situation for a proton is very interesting and forms the basis of the NMR technique. The proton, characterized by a net longitudinal magnetization, M_0 is under the influence of two different and mutually perpendicular magnetic fields, B_0 and B_1. As a result, it experiences an effective magnetic field, characterized by B_{eff}. such that $B_{\text{eff.}} = B_0 + B_1$ ($B_{\text{eff.}}$ is, therefore a vector addition of the individual vectors B_0 and B_1). By virtue of its spin and under the influence of $B_{\text{eff.}}$, the longitudinal magnetization M_0 undergoes a precessional motion around this net effective magnetic field. In an exactly identical manner, the magnetic field vector of a radio frequency (RF) pulse generated in an NMR experiment acts as B_1, tipping over the longitudinal magnetization M_0 towards the transverse plane, in the process *exciting* the spins. This net magnetization, now directed towards the transverse plane is termed as the *transverse* magnetization, M_1. The precessional motion of M_1 in a NMR or MRI experiment induces an alternating voltage in a receiving coil with a frequency that is equal to the Larmor frequency, ν; in the process of generating the desired *MR signal* [46]. The signal so produced in a NMR or MRI experiment undergoes a multitude of simulations and computer processing to finally generate an image that can be used either for chemical species identification or for clinical purposes.

Once the RF pulse is switched off, the transverse magnetization M_1, eventually relaxes back to its original longitudinal counterpart, M_0. This apparent switch occurs either via a spin-lattice (T_1) relaxation or via a spin-spin (T_2) relaxation. In a *longitudinal relaxation process*, the transverse magnetization M_1 decreases with time and eventually the MR signal dies out. Consequently, the longitudinal magnetization, M_0 is slowly restored along the external magnetic field, B_0. In the process, energy is released within the surroundings and hence the overall process is termed as *spin-lattice relaxation*. It is characterized by a time constant, T_1, which is independent of B_0 and the internal motion of molecules and ranges within 0.5–5 s. Alternatively, in the *transverse relaxation phenomenon*, all spins that are initially *in phase*, undergo mutual energy exchange together with contributions from inhomogeneity in B_0 (with an additional time constant, $T_2{}^*$) resulting in *de-phasing* and consequent decrease in M_1. As the energy exchange occurs within the spins, the overall process is termed as *spin-spin relaxation*. It is characterized by a time constant T_2 and ranges within 100–300 ms [47].

With a general idea of the physics behind the MRI experiment firmly established, let us now look at the various factors that can affect the image contrast. One of the most important factors is the *proton density* that is defined by the number of

excitable spins per unit volume. It determines maximum signal strength that can be emitted by tissue and can be tuned to obtain *proton-weighted* or *density-weighted* images. The *proton-weighted* images have a *higher signal-to-noise ratio* and are helpful to visualize bones and connective tissues. It is used to create high-resolution images and is extremely useful for clinical images of the brain, spinal cord as well as musculoskeletal system.

Other factors that contribute towards image contrast are the longitudinal relaxation time (T_1); a factor that decides how fast the spins would recover once disoriented by a small RF pulse. It can similarly be monitored to generate T_1-*weighted* images. The image contrast in a T_1-*weighted* experiment is influenced by a factor called the *repetition time*, T_R. T_R is defined as the time span between two successive excitations of the same slice and the experiment involves repeated excitation of the same tissue slice and consequent signal measurement to create an MR image. A short repetition time is characterized by a *high* T_1-*weighing* whereas long repetition times are characterized by *low* T_1-*weighing*. In a T_1-*weighted* image, tissues with *short* T_1 give *bright* images while tissues with *long* T_1 appear *dark*.

Another important factor that decides image contrast is the transversal relaxation time (T_2); a factor that is related to the time required for the decay of a NMR signal and can be modulated to generate T_2-*weighted* images. The influence of T_2 on image contrast is determined by a factor called the *echo time*, T_E. T_E is the time period between excitation and measurement of the MR signal. A short echo time is characterized by a *weak* T_2-*weighing* whereas long echo times are characterized by *strong* T_2-*weighing*. Consequently, with longer echo times, the contrast between tissues would be more pronounced. For a T_2-*weighted* image, tissues with short echo times give *dark* images while tissues with long echo times appear *bright*. Both the T_1 and T_2 parameters can be controlled to enhance the influence of proton density in MR images. All such factors are also influenced by *tissue type*, resulting in images with *distinct tissue to tissue contrast*.

In conclusion, *Image Contrast* in MRI is determined by the difference in signal intensity obtained from the tissues of interest. This contrast depends either upon *intrinsic* (body-related) or ***extrinsic*** (instrument related) factors. Signal intensity is influenced by factors such as proton density and T_1 or T_2 spin relaxation times. Contrast Agents are employed in MRI to improve the diagnostic information by increasing the signal intensity difference obtained from the diseased and healthy parts of ambient tissues of interest that are physiologically different [48].

5 MRI CAs: Mode of Action, Design, and General Considerations

The utility of MRI as a diagnostic tool is enhanced on administration of contrast agents prior to a MRI examination. Contrast agents are species that typically contain

a paramagnetic entity (e.g., metal ion, iron oxides, labeled zeolites) that influence/reduce the relaxation times (T_1 or T_2) of ambient tissue water protons. Consequently, these are classified as either T_1 or T_2 agents, depending upon whether they reduce T_1 or T_2 for the tissue water protons. A Contrast agent (CA) can affect the image contrast in a number of ways. The CA being employed can *influence the spin or proton density* that in turn can lead to changes in signal intensity. For example, a reduction in spin or proton density can lead to consequent signal loss. CAs can also *reduce* T_1*and* T_2 *relaxation times.* For T_1-weighted images, the relaxation of nearby protons can be accelerated resulting in an increase in MRI signal strength. This leads to *positive enhancement in image contrast* and such CAs are termed as *positive CAs.* For T_2*-weighted* images greater de-phasing introduced by some CAs induce reduction in T_2 values. CAs can also bring about *changes in susceptibility* that can affect local field inhomogeneity leading to reduced signal intensity. This leads to a phenomenon called the *negative contrast*, wherein the image brightness is considerably reduced. Most T_2 agents that produce such effects are also termed as *negative CAs.* In addition, CAs can also *reduce the proton signal* by shifting the resonance frequency by several hundred ppm leading to drastic changes in image contrast. Thus the proton signal intensity of the MR image is either increased or decreased on administration of a T_1 or T_2 agent. The terms T_1 and T_2 are inversely related to *relaxivity*, r (r is inversely proportional to T) which is defined as the efficiency of a contrast agent in terms of its ability to reduce the relaxation time (T) or coherently, increase the *relaxation rate* (r) of the tissue water protons. Consequently, two terms, r_1 and r_2, are subsequently defined that refer respectively to the *longitudinal* and *transverse relaxation rates* of the concerned tissue water protons.

An ideal contrast agent must therefore possess some essential attributes [49]. First and foremost, it must be highly efficient in enhancing the relaxation rates of nearby aqueous protons. This requires the CA to possess high values of *relaxivity*, r_1*or* r_2; a higher r value ensuring better interaction of the contrast agent with the surrounding protons. Another important advantage of compounds with high relaxivity is related to their ease of detection at lower doses and the ability to provide greater contrast. Additionally, an ideal CA must preferentially localize within the target tissue, leading to a highly specific in vivo relaxivity. It is therefore important that the relaxation rates of the target tissue be enhanced in comparison to other ambient tissues. The CA must also exhibit sufficient in vivo stability and a consequent lack of toxicity to be put into human use. Finally, it should be able to display rapid tissue clearance within hours of its administration to a patient. Most of the clinically approved CAs are complexes of heavy transition and inner transition metals, which are toxic in their native form. The toxicity of the free chelating ligand is also a matter of concern, provided the CA undergoes in vivo dissociation in presence of a host of other endogenous metal ions such as Ca(II) and Zn(II).

A large number of contrast agents are available that are exceedingly diverse in their chemical composition [50–55]. They can be mono-nuclear or poly-nuclear ligands complexed with a paramagnetic metal ion of choice; polymeric or macromolecular carriers (bonded covalently or non-covalently with a paramagnetic transition or inner-transition metal ion); superparamagnetic iron oxides; metalloporphyrins

(HOPO class of ligands); ^{13}C labeled species; Chemical exchange saturation transfer (CEST) contrast agents; aerosols and gases to name just a few. The various contrast agents can also be classified based on their mode of administration viz. intravenous, oral, rectal, and a less common mode wherein the contrast agent is inhaled as a gas (CT agent for brain and lung imaging). Additionally, they can also be classified as extracellular, organ-specific, and blood pool contrast agents.

One of the most promising class of CAs constitutes polyaminocarboxylate ligands complexed with a paramagnetic metal ion of choice, usually Gadolinium (Gd^{3+}). Metal ions that contain one or more unpaired electrons possess a magnetic moment and are termed as *paramagnetic*. When complexes containing such paramagnetic metal ions are placed in aqueous solutions, a magnetic interaction between the magnetic moment of the unpaired electrons of the paramagnetic metal ion and that of the protons of surrounding water molecules ensues, which affects the proton longitudinal (T_1) and transversal (T_2) relaxation times. CAs that comprise a central Gd^{3+} ion augment both the transversal as well as the longitudinal relaxation rates. However, the percentage enhancement in the latter (r_1 or $1/T_1$) is much higher and as a result, such CAs are visualized best with T_1-*weighted* scans [56]. The metal ion Gd^{3+} is paramagnetic (7 unpaired electrons) and consequently has a very high magnetic moment (7.9 BM). In addition, Gd^{3+} has a symmetric ground state that results in longer electron spin relaxation times (10^{-8}–10^{-9} s) and allows for streamlined transfer of magnetic information to surrounding water molecules [32, 57]. With such favorable physical properties, the concerned species containing a paramagnetic metal ion are very effective in reducing the T_1 and T_2 relaxation time of the water protons, which can ultimately lead to better contrast in MR images. Gd^{3+} in its native form is toxic (LD_{50} = 0.3–0.5 mmol/kg for rats) and is known to be retained in various organs such as bones, liver, and spleen [58]. It is henceforth, administered in vivo as a complex with a suitable organic ligand in doses ranging from 0.1–0.3 mmol/kg of the body weight. On complexation with suitable ligands, the resulting Gd^{3+}-chelates possess minimal toxicity (LD_{50} = 10 mm mol/kg in rats). Once administered to a patient, issues pertaining to the in vivo thermodynamic and kinetic stability of these complexes need to be addressed. It is extremely important that the complex remains intact and is resistant to transmetallation/transchelation reactions to the various endogenous metal ions such as Zn(II) and Ca(II) and a host of endogenous ligands such as glutamate and citrate that are present in ample quantities inside the body. The stability of such complexes has been extensively studied and it is now understood that the in vivo kinetic stability of Gd^{3+} chelates are more important than their thermodynamic stability [59, 60].

Most of the concerned ligands that have been used for complexation with Gd^{3+} have one of two basic core structures. One of them is the open-chain diethylenetriaminepentaacetic acid (DTPA) while the other is the closed macrocyclic cyclen ring 1,4,7,10-tetraazacyclododecanetetraacetic acid (DOTA). The two core structures are shown in Fig. 2.

The first MR contrast agent to be approved for human use (1988) was the acyclic DTPA (diethylenetriaminepentaacetic acid) derivative, Gd-DTPA (Magnevist Scherring). The first cyclen derivative to be put into human use was Gd-DOTA (Dotarem).

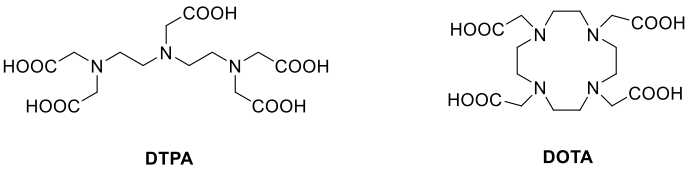

Fig. 2 The core structure of chelating ligands, DTPA and DOTA

Since then, a host of derivatives of both DTPA and DOTA have been studied as potential MR contrast agents. Both Magnevist and Dotarem along with a list of other CAs approved for clinical use in the United States are shown in Fig. 3.

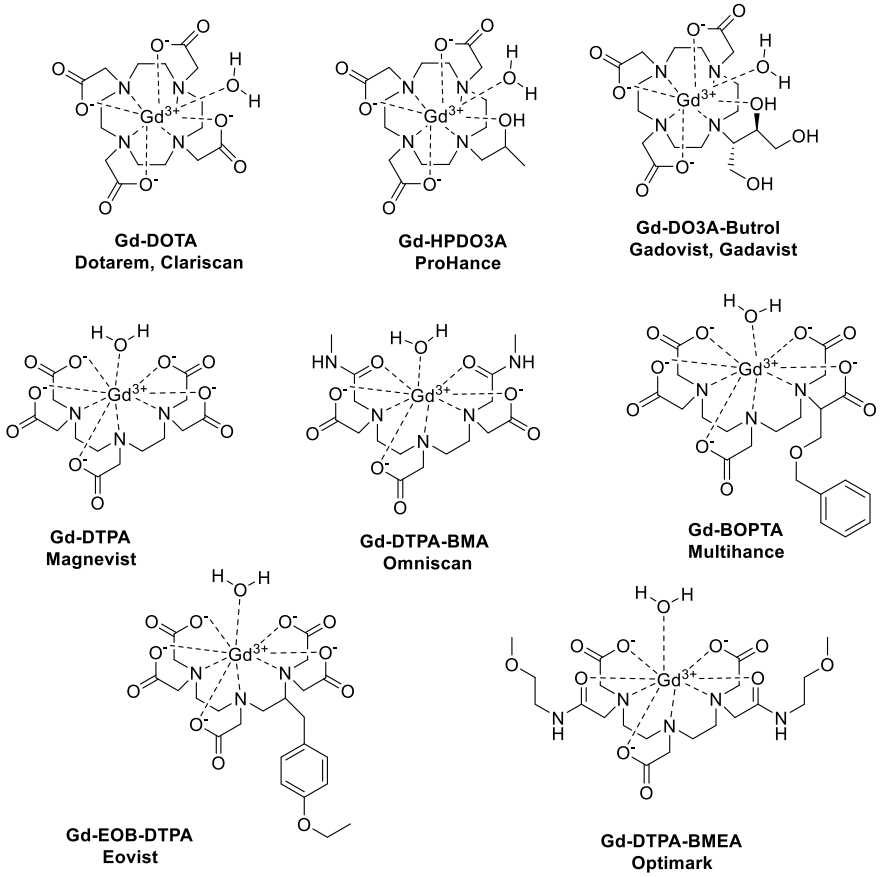

Fig. 3 MRI contrast agents approved for clinical use and currently sold in USA

About 40% of all MRI examinations performed around the world employ a *CA* such as a chelated paramagnetic Gd^{3+} ion. Such Gd^{3+} chelate systems must encompass a high thermo dynamic stability constant coupled with a miniscule metal dissociation rate, in addition to being hydrophilic and containing at least one coordinated water molecule available for rapid exchange with bulk water solvent. Enhanced T_1 relaxivity, r_1, is sought since the signal is brightened and the overall sensitivity is increased. Ongoing research involves efforts to enhance the relaxivity of contrast agents so as to obtain better resolution in the subsequent images, to achieve lower plasma clearance rates, and increase the specificity of these contrast agents. The successful design of a CA that ideally encompasses all the above attributes requires a thorough understanding of the behavior of such agents in aqueous solutions. As discussed beforehand, the Solomon-Bloembergen-Morgan (SBM) theory along with its various modifications provides a fundamental basis for such systems and considers all the possible interactions at interplay [61]. The following section presents a very basic treatise on the SBM theory, with special emphasis on the *points to remember* while designing such *ideal* CAs.

6 Contrast Agents and SBM Theory

The efficacy of a CA is determined in terms of its relaxivity, r_1 or r_2. The relaxivity of a CA is measured by its ability to enhance the relaxation rates of water protons at any given concentration, usually 1 mM. The observed relaxation rate of the water protons contains both a paramagnetic and a diamagnetic term. Mathematically, the relaxivity r_i $(i = 1, 2)$ is defined by Eq. 1 and can be described as the slope of a plot of the observed relaxation rate $(1/T_i)_{\text{obs.}}$ and the concentration of the CA, represented by the term [Gd].

$$(1/T_i)_{\text{obs.}} = (1/T_i)_{\text{dia.}} + r_i[\text{Gd}] \tag{1}$$

In Eq. 1, the paramagnetic contribution is the second term on the right-hand side and is linearly related to the concentration of the concerned paramagnetic entity. The increase in paramagnetic relaxation can be attributed to both an *inner-sphere* as well as an *outer-sphere* contribution. The *inner-sphere* term consists of the contribution to the proton relaxation from a solvent molecule directly coordinated with the Gd^{3+} ion. Such solvent molecules belong to the first coordination sphere of the complex. Similarly, the *outer sphere* term relates to an identical contribution from solvent molecules in the second coordination sphere of the complex as well as to those in the bulk solvent. The ability of the central Gd^{3+} ion to influence the overall relaxivity depends on the strength of such interaction with nearby solvent species. This interaction is inversely proportional to the distance between the concerned species and thus the contribution of the solvent molecules closest to the Gd^{3+} ion, i.e., those within the first coordination sphere of the complex are extremely important. This contribution enhances the longitudinal, inner sphere relaxivity, r_{1p}. Another important factor

relates to the *rate of solvent or water exchange* with the paramagnetic Gd^{3+} species. A faster exchange rate leads to a greater swap of magnetic information with the neighboring solvent molecules and this augments the resultant relaxivity. The exchange rate is characterized by the *mean water residence time*, τ_M and should have small values for a faster exchange rate. Equation 2 relates these factors mathematically to the paramagnetic proton relaxation enhancement;

$$1/T_1 = q P_m[1/(T_{1m} + \tau_M)] \tag{2}$$

In Eq. 2, the term $1/T_1$ refers to the longitudinal relaxation rate, q refers to the total number of solvent water molecules present in the first coordination sphere of the Gd-complex, while P_m and $1/T_{1m}$ refer to the mole fraction and the relaxation rate of water or solvent molecule coordinated to the Gd^{3+} center, respectively. According to the SBM theory and the related mathematical equations, the term $1/T_{1m}$ is governed by the dipole-dipole relaxation mechanism and is critically influenced by the *correlation time*, τ_{ic} $(i = 1, 2)$ of the molecular tumbling motion, defined mathematically by Eq. 3;

$$1/\tau_{ci} = 1/\tau_R + 1/T_{ie} + 1/\tau_M \tag{3}$$

In Eq. 3, τ_R refers to the *rotational correlation time* and signifies the extent of rotation or tumbling undergone by the Gd-complex. The term T_{ie} refers to the electronic *relaxation time*. The correlation time takes into account the alterations in the local magnetic field brought about by the tumbling motion of the complex and has to achieve optimum values for the desired high relaxivity of a CA.

In a nutshell, the SBM theory and its modifications relate to a number of factors that can influence the relaxivity of a CA. These factors can be colligated with ligand structure, design, and the overall motion of a CA when put into a solution. The three most important factors that affect the relaxivity attained by a complex are, the number of directly coordinated water molecules to the central metal ion (q); the residence time of a water molecule coordinated to the metal center (τ_M) and the rotational correlation time that measures the extent of rotation or tumbling undergone by a complex (τ_R). In addition, there are spates of electronic interactions especially with the water molecules in the outer coordination sphere of the complex that also affect the relaxivity for a contrast agent, although to a much lesser extent.

The current batch of CAs approved for clinical use are based on a central Gd^{3+} ion that is chelated to either an open-chain or a macrocyclic polyamino polycarboxylic acid ligand. For all such ligands, based on either the DTPA or DOTA framework (Fig. 2), the number of available ligation sites is eight. The central Gd^{3+} ion, however, has a coordination number of nine and hence for such clinically approved Gd-DTPA or a Gd-DOTA system, only one coordination site on Gd^{3+} is left for direct coordination with a water molecule. For these complexes, the value of q is 1. This coordinated water molecule is rapidly exchanged with the surrounding solvent water molecules and brings about the relaxation pertinent to these complexes. For complexes with larger q values, the extent of exchange of the coordinated water molecule with the surrounding solvent water molecules increases, and so does the

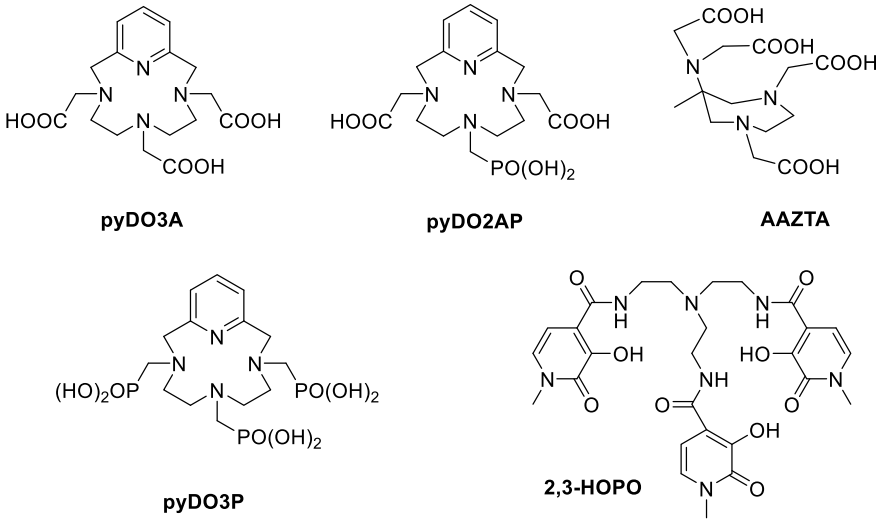

Fig. 4 Six and Seven coordinate ligands for conjugation with Gd^{3+} ion

relaxivity. However, with more water molecules directly coordinated with the central Gd^{3+} ion, the number of ligation sites left for the ligand attachment decreases and consequently the stability of the overall complex is drastically compromised. Ligands with seven and six coordination sites have been designed (Fig. 4) and corresponding Gd^{3+} complexes with $q = 2$ and 3 have been synthesized [62]. These complexes report higher relaxivity than Gd-DTPA or Gd-DOTA complexes, but their thermodynamic and kinetic stability profiles are not favorable and hence these have not been approved for clinical use, in spite of a promising relaxivity profile. Again, these complexes are also known to undergo dimer/trimer formation with the central metal ion [63, 64]. This decreases the q value for these complexes and consequently the gain in relaxivity is compromised.

The optimal values for τ_M and τ_R are both 10 ns at a magnetic field strength of 1.5 T [65]. For the various contrast agents put into clinical use, values attained for τ_M and τ_R are 100 ns and 0.1 ns, respectively. Clearly, there is an urgent need to optimize these values by designing complexes with a more favorable τ_M and τ_R. In principle, contrast agents with ligands having a more globular structure are bound to decrease the rotational tumbling of the resulting complex and therefore can bring about an increase in τ_R. Another strategy to enhance τ_R is to link up multiple DTPA/DOTA complexes with a suitable carrier, i.e., design a contrast agent with a *high pay load* [52, 66]. For optimization of τ_M values, various strategies can be undertaken. For example, it is known that complexes with an overall negative charge decrease the residence time of coordinated water molecules as compared to complexes that are neutral. Similarly, introduction of side chains in the pendant arms, especially replacement of acetate groups with bulkier phosphate groups, replacing carbon atoms in the core structure of DTPA and DOTA and introduction of greater

steric constraints within the binding sites of the ligands can affect the residence time of water molecules [67–69]. All these strategies to improve ligand design have been extensively reviewed and constitute the bulk of research pertaining to the search for the so-called *ideal* contrast agents.

7 Details for Clinically Approved MRI Contrast Agents

As explained previously, clinically approved MRI contrast agents can be divided into acyclic, open-chain Gd-chelates and macrocyclic, closed chain Gd-chelates. We will briefly discuss each of these agents individually followed by future outlooks [70].

7.1 Magnevist

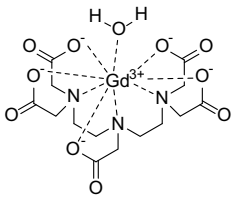

Gd-DTPA, Magnevist

Magnevist (Gd-DTPA, Gadopentate dimeglumine) was the first MRI CA approved for clinical use in 1988 as an extracellular fluid agent. It is an open chain, acyclic Gd-chelate that is used for detection of lesions with abnormal vascularity in the brain (intracranial lesions), spine, and associated tissues. It is also utilized for visualizing abnormalities in the body (excluding the heart), head, and neck. Upon IV injection, Magnevist undergoes non-specific biodistribution and is eliminated via the kidneys. It is marketed as single-dose vials, prefilled single-dose injections, and pharmacy bulk packages a clear, colorless to slightly yellow solution containing 0.5 mmol gadopentetate dimeglumine/mL (equivalent to 469.01 mg/mL of gadopentetate dimeglumine) for intravenous use.

As of September 2019, Magnevist will no longer be provided as an injection by its supplier (Bayer) to the United States. This is in response to the shift towards greater use of macrocyclic Gd-chelates in the clinics and a consequent reduction in use of open-chain agents [71].

7.2 Omniscan

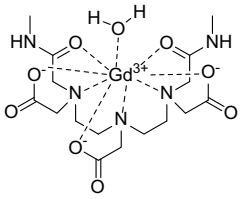

Gd-DTPA-BMA, Omniscan

Omniscan (Gd-DTPA-BMA, gadodiamide) was the second open chain, acyclic MRI CA approved for clinical use in 1993 as an extracellular fluid agent. It is approved as an intravenous injection for the detection of abnormalities in vasculature in the brain, spine, thoracic (non-related to heart), abdominal, pelvic cavities, retroperitoneal space and associated tissues. On IV injection, Omniscan undergoes non-specific biodistribution and is eliminated via the kidneys. It is marketed as single dose vials, prefilled injections and pharmacy bulk packages as a sterile aqueous solution for intravenous injection (287 mg/mL) bolus intravenous use.

As of July 20, 2017, the European Medicine Agency (EMA) has recommended the suspension of Omniscan for MRI exams in the European Union (EU) [72]. This is a direct consequence of concerns regarding the deposition of Gd in the brain tissues for patients who have undergone linear Gd-chelate assisted MRI. There are also additional concerns due to NSF in patients with impaired renal function.

7.3 Optimark

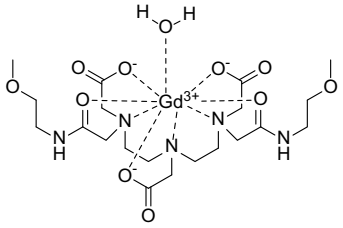

Gd-DTPA-BMEA, Optimark

Optimark (Gd-DTPA-BMEA, gadoversetamide) was the third open chain, acyclic MRI CA approved for clinical use in 1999 as an extracellular fluid agent. It was developed for MRI of the central nervous system and liver. It has also been approved for use in patients with abnormalities in vasculature of the spine, brain, the blood brain barrier (BBB), and associated tissues. It is a non-ionic species and henceforth

has a lower osmolality than ionic agents such as Magnevist. Optimark undergoes non-specific biodistribution and is cleared through renal excertion (urine) on IV administration. It is marketed as glass vials and prefilled injections as a clear, colorless to slightly yellow solution for injection containing 330.9 mg gadoversetamide per mL (equivalent to 0.5 mmol/mL) sterile aqueous solution for intravenous injection.

As of July 20, 2017, the European Medicine Agency (EMA) has also recommended the suspension of Optimark for MRI exams in the European Union (EU) [72]. This is again a consequence of concerns regarding the deposition of Gd in the brain tissues for patients who have undergone linear Gd-chelate assisted MRI. There are also additional concerns due to NSF in subjects with renal dysfunction.

7.4 Multihance

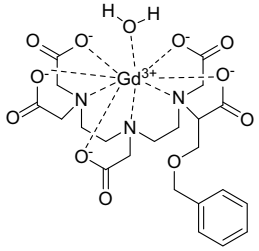

Gd-BOPTA, Multihance

Multihance (Gd-BOPTA, gadobenate dimeglumine) was the fourth open chain, acyclic MRI CA approved for clinical use in 2004 as an extracellular fluid agent. Multihance was originally developed for potential hepatobiliary distribution, however, it was realized that its biodistribution is species-specific. Thus, in mice and rats, Multihance undergoes about 50% clearance by the liver while in human subjects only 2–5% clearance is observed through the hepatobiliary route and the rest of the administered dose is cleared through the kidneys. Multihance also undergoes non-specific and transient interactions with macromolecules, resulting in increase in the overall size and consequent slower tumbling rate leading to higher r_1 and r_2 relaxivity in solutions containing serum proteins. MultiHance is a linear, ionic species and has a higher osmolality than plasma and is hypertonic under conditions of use. It is marketed in single-use glass vials a clear, colorless solution containing 529 mg gadobenate dimeglumine per mL.

Although there are concerns with free Gd-associated toxicity with Multihance use, EMA has suggested its continuation for liver MRI scans due to its somewhat liver-specific uptake and related importance in diagnosis of liver lesions in the EU [72].

7.5 Eovist

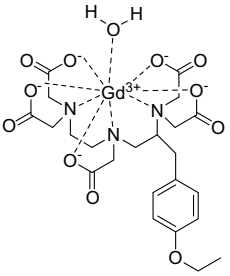

Gd-EOB-DTPA, Eovist

Eovist (Gd-EOB-DTPA, disodium gadoxetic acid) was the fifth open chain, acyclic MRI CA approved for clinical use in 2008 in the United States as a liver-specific MRI CA. Prior to this, the agent was already approved under the trade name Primovist in Europe in the year 2005 as a hepatobiliary contrast agent for MRI. The lipophilic ethoxybenzyl moiety within Gd-EOB-DTPA is unique to its structure and is responsible for liver-specific uptake. Once injected i.v., Eovist is rapidly taken up by both the liver and the kidneys and is subsequently excreted by the hepatobiliary (~50%) and renal (~50%) route. Interestingly, the hepatocyte cells in the liver drive the uptake of Eovist in it and this allows for delineation between healthy and tumorous liver tissues due to preferential uptake of Eovist by the neoplastic cells. Eovist is a linear, anionic charged species that exhibits low protein binding and has higher osmolality than plasma. It is marketed in single-use glass vials as a clear, colorless solution-containing 181.43 mg/mL of gadoxetate disodium, equivalent to 0.25 mmol/mL.

Similar to other open-chain Gd-chelates, free Gd-associated toxicity is a concern for Eovist. However, due to its specificity for delineation of liver lesions, it is used for analysis in patients with related disease scenarios.

7.6 Dotarem

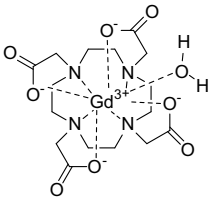

Gd-DOTA, Dotarem, Clariscan

Dotarem (Gd-DOTA, gadoterate meglumine) was the first macrocyclic, ionic MRI CA approved for clinical use in 1989 in Europe and was approved by FDA in 2013 for use in the United States for visualization of abnormalities in the brain, spine, and surrounding tissues. Clariscan is the generic version of Dotarem that was approved in 2019 for clinical use in the United States. In subjects with a compromised BBB and abnormalities in vasculature, Dotarem administration allows for detection of lesions such as neoplasm, infarcts, or abscesses. Upon i.v. administration, Dotarem is rapidly distributed in the extracellular space and is eliminated primarily through the kidneys and urine. It is marketed in single-use glass vials and pre-filled syringes a sterile, nonpyrogenic, clear, colorless to yellow, aqueous solution of 0.5 mmol/mL containing 376.9 mg/mL gadoterate meglumine.

A major advantage of macrocyclic MRI CAs as compared to their open-chain counterparts is their enhanced thermodynamic and kinetic stability. As a result, these are now the preferred agents for clinical use. Multiple reports have indicated their safety in terms of Gd release and they have emerged as a viable option for MRI contrast exams in patients with renal failure.

7.7 ProHance

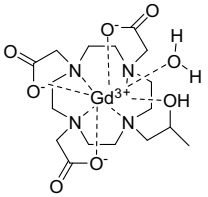

Gd-HPDO3A, ProHance

ProHance (Gd-HP-DO3A, gadoteridol) was the second macrocyclic MRI CA approved for clinical use in 1992 as an extracellular fluid agent for the non-targeted imaging of lesions in the CNS and extracranial/extraspinal tissues. ProHance is a non-ionic species that has a lower osmolality than agents such as Gd-DTPA but a higher Gd to solute particle ratio. The mechanism of action for ProHance pertains to the enhanced contrast observed in patients with a compromised BBB and perfusion deficiency in extracranial/extraspinal tissues as compared to patients with an intact BBB and associated tissue framework. Similar to the other macrocyclic CA Dotarem, upon i.v. administration, ProHance is rapidly distributed in the extracellular space and is eliminated primarily through the kidneys and urine. It is marketed in single-use glass vials and pre-filled syringes as a clear, colorless to slightly yellow solution containing 279.3 mg/mL of gadoteridol.

Again, similar to Dotarem, ProHance being a macrocyclic MRI CAs enjoys higher thermodynamic and kinetic stability as compared to their open-chain counterparts.

Thus, they have emerged as a viable option for MRI contrast exams in patients with renal failure.

7.8 Gadovist

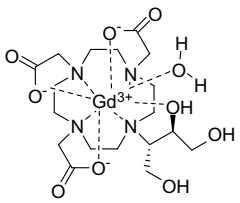

Gd-DO3A-Butrol, Gadovist, Gadavist

Gadovist (Gd-DO3A-Butrol, gadobutrol) was the third macrocyclic MRI CA approved for clinical use in 1998 in Europe and in 2011 in the United States (trade name Gadavist) as an extracellular fluid (ECF) agent for non-targeted imaging of the blood pool. Akin to other ECF agents, Gadovist does not cross an intact BBB. However, for subjects with a compromised BBB or the lack of it in the pituitary gland, meningiomas, or tumor margins, CNS lesions are clearly delineated following i.v. administration of Gadovist. The trihydroxybutyl group in Gadovist was introduced to enhance the overall hydrophilicity of the resulting chelate leading to lower protein binding and higher in vivo tolerance. Although a non-ionic species, the Gadovist formulation displays higher osmolality than the ionic Dotarem and the neutral ProHance. Following i.v. administration, Gadovist is rapidly distributed in the extracellular space and is excreted via kidneys. It is marketed in single-use glass vials and pre-filled syringes as a clear, colorless to pale yellow solution containing 1 mmol gadobutrol (equivalent to 604.72 mg gadobutrol) per mL as the active ingredient. Again, similar to Dotarem and ProHance, Gadovist exhibits higher thermodynamic and kinetic stability as compared to their open-chain counterparts and has emerged as a viable option for MRI contrast exams in patients with renal failure.

8 MRI-Clinical Applications

MRI has revolutionized the field of clinical imaging [73]. Conventional MRI is used in the clinics for functional and morphological characterization of a patient. For example, MRI has slowly developed as a method of choice for cardiovascular imaging. Several improvements in spin-echo techniques that provide access to various contrast mechanisms are now being used to delineate subtle abnormalities in cardiac function and flow, changes in cardiovascular morphology, myocardial

viability and perfusion as well as coronary MR angiography. Another excellent use of MRI refers pertains to the mapping of clinical as well as experimental cerebral ischemia. Over the years, improvements in MRI scanner hardware, pulse sequence, and user interface have positioned it a technique of choice for image guidance in interventional procedures. MRI provides for unmatched soft tissue contrast even without the use of exogenous contrast media and this can aid tremendously in the delineation of target lesions. As the MRI does not use any harmful radiation, the damage to surrounding tissue anatomy is non-existent when compared to other techniques such as CT and PET. Further, by using various pulse sequences subtle differences in normal and damaged tissue can be visualized to obtain a plethora of functional information that is of critical importance to determine the end-point of a surgical intervention. MRI can also aid in thermal ablation procedures by monitoring temperature changes in tissues. Dynamic MR Mammography (MRM), a technique that combines a dedicated breast coil and a rapid 2D gradient-echo imaging sequence together with a bolus injection of GBCA is considered a prominent diagnostic tool for breast cancer imaging. It is an excellent technique to measure disease extent, presence of absence of malignancy, and evaluation of tumor response to neoadjuvant chemotherapy. Another interesting aspect of MRI relates to MR Spectroscopy (MRS) that can be used to study the metabolism of tissues and organs of interest, especially the tumor biochemistry that can be of utmost importance to determine prognosis and response to treatment for the subject of interest.

9 Future Directions and Conclusions

Despite several years of research and development, most clinically used low molecular weight MRI CAs suffer from some basic disadvantages, namely relatively low r_1 values (~4 s^{-1} mM^{-1} at higher magnetic field strength), lack of selectivity for tissues and extremely short intravascular half-lives (~20 min) [74]. Moreover, such low molecular weight CAs do not provide sufficient contrast at low concentrations, which is essential for biomedical and targeted imaging [75]. Till recently, GBCAs were considered to be the safest pharmaceutical agents barring very few short and long-term adverse effects [76]. However, this situation dramatically changed in 2006, when reports about a potentially fatal, new disease condition called Nephrogenic Systemic Fibrosis (NSF) was reported in patients with impaired renal function [77, 78]. Over the years, there have also been reports of long-term Gadolinium retention in the body following repeated administration of GBCAs [79]. Fortunately, the condition of NSF has only been reported for the usage of open chain, acyclic GBCAs that have with lower thermodynamic and kinetic stability than their macrocyclic, closed chain counterparts and are thus subject to Gd loss due to chelation with endogenous cations [Ca(II), Zn(II), etc.) and anions (citrate, glutamate, etc.) [80, 81]. This has led to the subsequent suspension of the use of open chain GBCAs, Magnevist, Omniscan, and Optimark by the European Medicines Agency (EMA) in the EU. Recently, Magnevist was also taken off from the market in the US due to potential

toxicity concerns. Thus, there has been a renewed interest in the investigation of alternatives to GBCAs for MRI, which is now an active area of research. It must be emphasized that the design, synthesis, and potential human administration of a contrast agent requires a thorough understanding of the underlying principles of contrast generation in MRI, chelate chemistry, solution thermodynamics and kinetics, pharmacology, biodistribution, and the pertaining economics of the manufacturing process. Efforts are certainly underway in this direction and this would require active collaboration and exchange of ideas between chemists, biochemists, physicists, and clinicians.

References

1. Chakravarty, S.: Closomers at a click: a treatise on the design, synthesis and in vivo MRI of novel click closomers as high performance and efficacious contrast agents. University of Missouri, Columbia (2013)
2. Peregrinus, P.: Epistola Petri Peregrini de Maricourt ad Sygerum de Foucaucourt, Militem, De Magnete. Privately Published, Italy (1269)
3. Gilbert, W.: De Magnete, Magneticisque, Corporibus, et de Magno Magnete Tellure; Physiologica Nova (On the lodestone, magnetic bodies, and on the great magnet the earth). Dover (Paperback republication, 1991, Translation: Mottelay, P.F.), New York (1600)
4. Mourino, M.R.: From Thales to Lauterbur, or from the lodestone to MR imaging: magnetism and medicine. Radiology **180**, 593–612 (1991). https://doi.org/10.1148/radiology.180.3.1871268https://doi.org/10.1148/radiology.180.3.1871268
5. Mitchell, A.C.: Chapters in the history of terrestrial magnetism. Terr. Magn. Atmos. Electr. **44**, 77–80 (1939). https://doi.org/10.1029/TE044i001p00077https://doi.org/10.1029/TE044i001p00077
6. Häfeli, U.: The history of magnetism in medicine. In: Magnetism in Medicine, pp. 1–25 (2006)
7. Macklis, R.M.: Magnetic healing, quackery, and the debate about the health effects of electromagnetic fields. Ann. Int. Med. **118**, 376–383 (1993). https://doi.org/10.7326/0003-4819-118-5-199303010-00009https://doi.org/10.7326/0003-4819-118-5-199303010-00009
8. Lord Butterfield of Stechford: Dr Gilbert's magnetism. Lancet **338**, 1576–1579 (1991). https://doi.org/10.1016/0140-6736(91)92388-I
9. Shermer, M.: Mesmerized by magnetism. Sci. Am. **287** (2002)
10. Livingston, J.D.: Driving force: the natural magic of magnets, 1st edn. Harvard University Press, Cambridge (1996)
11. Asti, G., Solzi, M.: Permanent magnets. In: Gerber, R., Wright, C.D., Asti, G. (eds.) Applied Magnetism, pp. 309–375. Springer, Dordrecht (1994)
12. Hilai, S.K., Jost Michelsen, W., Driller, J., Leonard, E.: Magnetically guided devices for vascular exploration and treatment. Radiology **113**, 529–540 (1974). https://doi.org/10.1148/113.3.529https://doi.org/10.1148/113.3.529
13. Ram, W., Meyer, H.: Heart catheterization in a neonate by interacting magnetic fields: a new and simple method of catheter guidance. Cathet. Cardiovasc. Diagn **22**, 317–319 (1991). https://doi.org/10.1002/ccd.1810220412https://doi.org/10.1002/ccd.1810220412
14. McNeil, R.G., Ritter, R.C., Wang, B., et al.: Characteristics of an improved magnetic-implant guidance system. IEEE Trans. Biomed. Eng. **42**, 802–808 (1995). https://doi.org/10.1109/10.398641https://doi.org/10.1109/10.398641
15. Poznansky, M.J., Juliano, R.L.: Biological approaches to the controlled delivery of drugs: a critical review. Pharmacol. Rev. **36**, 277–336 (1984)
16. Rand, R.W., Snyder, M., Elliott, D., Snow, H.: Selective radiofrequency heating of ferrosilicone occluded tissue: a preliminary report. Bull. Los Angeles Neurol. Soc. **41**, 154–159 (1976)

17. Sako, M., Hirota, S., Morita, M., et al.: Clinical evaluation of ferromagnetic microembolization in the treatment of hepatoma. Nihon Gan Chiryo Gakkai Shi **20**, 1317–1326 (1985)
18. Chan, D.C.F., Kirpotin, D.B., Bunn, P.A.: Synthesis and evaluation of colloidal magnetic iron oxides for the site-specific radiofrequency-induced hyperthermia of cancer. J. Magn. Magn. Mater. **122**, 374–378 (1993). https://doi.org/10.1016/0304-8853(93)91113-L
19. Jordan, A., Scholz, R., Maier-Hauff, K., et al.: Presentation of a new magnetic field therapy system for the treatment of human solid tumors with magnetic fluid hyperthermia. J. Magn. Magn. Mater. **225**, 118–126 (2001). https://doi.org/10.1016/S0304-8853(00)01239-7
20. Gneveckow, U., Jordan, A., Scholz, R., et al.: Description and characterization of the novel hyperthermia- and thermoablation-system for clinical magnetic fluid hyperthermia. Med. Phys. **31**, 1444–1451 (2004). https://doi.org/10.1118/1.1748629https://doi.org/10.1118/1.1748629
21. Maier-Hauff, K., Rothe, R., Scholz, R., et al.: Intracranial thermotherapy using magnetic nanoparticles combined with external beam radiotherapy: results of a feasibility study on patients with glioblastoma multiforme. J. Neurooncol. **81**, 53–60 (2007). https://doi.org/10.1007/s11060-006-9195-0https://doi.org/10.1007/s11060-006-9195-0
22. Wahsner, J., Gale, E.M., Rodríguez-Rodríguez, A., Caravan, P.: Chemistry of MRI contrast agents: current challenges and new frontiers. Chem. Rev. **119**, 957–1057 (2019). https://doi.org/10.1021/acs.chemrev.8b00363https://doi.org/10.1021/acs.chemrev.8b00363
23. Pysz, M.A., Gambhir, S.S., Willmann, J.K.: Molecular imaging: current status and emerging strategies. Clin. Radiol. **65**, 500–516 (2010). https://doi.org/10.1016/j.crad.2010.03.011
24. Glover, G.H.: Overview of Functional Magnetic Resonance Imaging. Neurosurg. Clin. N. Am. **22**, 133–139 (2011). https://doi.org/10.1016/j.nec.2010.11.001
25. Runge, V.M.: Critical questions regarding gadolinium deposition in the brain and body after injections of the gadolinium-based contrast agents, safety, and clinical recommendations in consideration of the EMA's pharmacovigilance and risk assessment committee recommend. Invest. Radiol. **52**, 317–323 (2017). https://doi.org/10.1097/RLI.0000000000000374https://doi.org/10.1097/RLI.0000000000000374
26. Doan, B.-T., Meme, S., Beloeil, J.-C.: General principles of MRI. Chem. Contrast Agents Med. Magn. Reson. Imaging 1–23 (2013)
27. Bloch, F., Hansen, W.W., Packard, M.: The nuclear induction experiment. Phys. Rev. **70**, 474–485 (1946). https://doi.org/10.1103/PhysRev.70.474https://doi.org/10.1103/PhysRev.70.474
28. Solomon, I.: Relaxation processes in a system of two spins. Phys. Rev. **99**, 559–565 (1955). https://doi.org/10.1103/PhysRev.99.559https://doi.org/10.1103/PhysRev.99.559
29. Bloembergen, N.: Proton relaxation times in paramagnetic solutions. J. Chem. Phys. **27**, 572–573 (1957). https://doi.org/10.1063/1.1743771https://doi.org/10.1063/1.1743771
30. Lipari, G., Szabo, A.: Model-free approach to the interpretation of nuclear magnetic resonance relaxation in macromolecules. 1. Theory and range of validity. J. Am. Chem. Soc. **104**, 4546–4559 (1982a). https://doi.org/10.1021/ja00381a009https://doi.org/10.1021/ja00381a009
31. Lipari, G., Szabo, A.: Model-free approach to the interpretation of nuclear magnetic resonance relaxation in macromolecules. 2. Analysis of experimental results. J. Am. Chem. Soc. **104**, 4559–4570 (1982b). https://doi.org/10.1021/ja00381a010https://doi.org/10.1021/ja00381a010
32. Banci, L., Bertini, I., Luchinat, C.: Nuclear and Electron Relaxation. VCH, Weinheim (1991)
33. Eisinger, J., Shulman, R.G., Blumberg, W.E.: Relaxation enhancement by paramagnetic ion binding in deoxyribonucleic acid solutions. Nature **192**, 963–964 (1961). https://doi.org/10.1038/192963a0https://doi.org/10.1038/192963a0
34. Lauterbur, P.C.: Image formation by induced local interactions: examples employing nuclear magnetic resonance. Nature **242**, 190–191 (1973). https://doi.org/10.1038/242190a0https://doi.org/10.1038/242190a0
35. Mansfield, P., Maudsley, A.A.: Planar spin imaging by NMR. J. Magn. Reson. **27**, 101–119 (1977). https://doi.org/10.1016/0022-2364(77)90197-4
36. Hinshaw, W.S., Bottomley, P.A., Holland, G.N.: Radiographic thin-section image of the human wrist by nuclear magnetic resonance. Nature **270**, 722–723 (1977). https://doi.org/10.1038/270722a0https://doi.org/10.1038/270722a0

37. Pykett, I.L., Hinshaw, W.S., Buonanno, F.S., et al.: Physical principles of NMR imaging. Curr. Probl. Cancer **7**, 37–50 (1982). https://doi.org/10.1016/S0147-0272(82)80009-3
38. Lauterbur, P.C.: NMR zeugmatographic imaging in medicine. J. Med. Syst. **6**, 591–597 (1982). https://doi.org/10.1007/BF00995509https://doi.org/10.1007/BF00995509
39. Brady, T.J., Goldman, M.R., Pykett, I.L., et al.: Proton nuclear magnetic resonance imaging of regionally ischemic canine hearts: effect of paramagnetic proton signal enhancement. Radiology **144**, 343–347 (1982). https://doi.org/10.1148/radiology.144.2.6283594https://doi.org/10.1148/radiology.144.2.6283594
40. Young, I.R., Clarke, G.J., Baffles, D.R., et al.: Enhancement of relaxation rate with paramagnetic contrast agents in NMR imaging. J. Comput. Tomogr. **5**, 543–547 (1981). https://doi.org/10.1016/0149-936X(81)90089-8
41. Carr, D.H., Brown, J., Bydder, G.M., et al.: Intravenous chelated gadolinium as a contrast agent in NMR imaging of cerebral tumors. Lancet **323**, 484–486 (1984). https://doi.org/10.1016/S0140-6736(84)92852-6
42. Carr, D.H., Brown, J., Bydder, G.M., et al.: Gadolinium-DTPA as a contrast agent in MRI: initial clinical experience in 20 patients. Am. J. Roentgenol. **143**, 215–224 (1984). https://doi.org/10.2214/ajr.143.2.215https://doi.org/10.2214/ajr.143.2.215
43. Clare, S.: Functional MRI: Methods and Applications. University of Nottingham (1997)
44. Vlaardingerbroek, M.T., den Boer, J.A.: Magnetic Resonance Imaging. Springer, Berlin (2003)
45. Dale, B.M., Brown, M.A., Semelka, R.C.: Instrumentation. In: Dale, B.M., Brown, M.A., Semelka, R.C. (eds.) MRI Basic Principles and Applications, pp. 177–188 (2015)
46. Smith, R.C., Lange, R.C.: Understanding Magnetic Resonance Imaging, 1st edn. CRC Press, New York (1997)
47. Weishaupt, D., Köchli, V.D., Marincek, B.: How Does MRI Work? An Introduction to the Physics and Function of Magnetic Resonance Imaging, 2nd edn. Springer, Berlin (2006)
48. Geraldes, C.F.G.C., Laurent, S.: Classification and basic properties of contrast agents for magnetic resonance imaging. Contrast Media Mol. Imaging **4**, 1–23 (2009). https://doi.org/10.1002/cmmi.265https://doi.org/10.1002/cmmi.265
49. Hao, D., Ai, T., Goerner, F., et al.: MRI contrast agents: basic chemistry and safety. J. Magn. Reson. Imaging **36**, 1060–1071 (2012). https://doi.org/10.1002/jmri.23725https://doi.org/10.1002/jmri.23725
50. Tóth, É., Helm, L., Merbach, A.E.: Relaxivity of MRI contrast agents. In: Krause, W. (ed.) Contrast Agents I: Magnetic Resonance Imaging, pp. 61–101. Springer, Berlin (2002)
51. Muller, R.N., Vander Elst, L., Roch, A., et al.: Relaxation by Metal-Containing Nanosystems, pp. 239–292. Academic Press (2005)
52. Chan, K.W.-Y., Wong, W.-T.: Small molecular gadolinium(III) complexes as MRI contrast agents for diagnostic imaging. Coord. Chem. Rev. **251**, 2428–2451 (2007). https://doi.org/10.1016/j.ccr.2007.04.018
53. Werner, E.J., Datta, A., Jocher, C.J., Raymond, K.N.: High-relaxivity MRI contrast agents: where coordination chemistry meets medical imaging. Angew. Chem. Int. Ed. **47**, 8568–8580 (2008). https://doi.org/10.1002/anie.200800212https://doi.org/10.1002/anie.200800212
54. Viswanathan, S., Kovacs, Z., Green, K.N., et al.: Alternatives to gadolinium-based metal chelates for magnetic resonance imaging. Chem. Rev. **110**, 2960–3018 (2010). https://doi.org/10.1021/cr900284ahttps://doi.org/10.1021/cr900284a
55. Zhou, Z., Lu, Z.R.: Gadolinium-based contrast agents for magnetic resonance cancer imaging. WIREs Nanomed. Nanobiotechnol. **5**, 1–18 (2013). https://doi.org/10.1002/wnan.1198https://doi.org/10.1002/wnan.1198
56. Caravan, P., Ellison, J.J., McMurry, T.J., Lauffer, R.B.: Gadolinium(III) chelates as MRI contrast agents: structure, dynamics, and applications. Chem. Rev. **99**, 2293–2352 (1999). https://doi.org/10.1021/cr980440xhttps://doi.org/10.1021/cr980440x
57. Koenig, S.H., Brown, R.D., III., Spiller, M., Lundbom, N.: Relaxometry of brain: why white matter appears bright in MRI. Magn. Reson. Med. **14**, 482–495 (1990). https://doi.org/10.1002/mrm.1910140306https://doi.org/10.1002/mrm.1910140306

58. McDonald, R.J., Levine, D., Weinreb, J., et al.: Gadolinium retention: a research roadmap from the 2018 NIH/ACR/RSNA workshop on gadolinium chelates. Radiology **289**, 517–534 (2018). https://doi.org/10.1148/radiol.2018181151https://doi.org/10.1148/radiol.2018181151
59. Hermann, P., Kotek, J., Kubíček, V., Lukeš, I.: Gadolinium(iii) complexes as MRI contrast agents: ligand design and properties of the complexes. Dalt. Trans. 3027–3047 (2008). https://doi.org/10.1039/B719704G
60. Clough, T.J., Jiang, L., Wong, K.L., Long, N.J.: Ligand design strategies to increase stability of gadolinium-based magnetic resonance imaging contrast agents. Nat. Commun. **10**, 1420 (2019). https://doi.org/10.1038/s41467-019-09342-3https://doi.org/10.1038/s41467-019-09342-3
61. De León-Rodríguez, L.M., Martins, A.F., Pinho, M.C., et al.: Basic MR relaxation mechanisms and contrast agent design. J. Magn. Reson. Imaging **42**, 545–565 (2015). https://doi.org/10.1002/jmri.24787https://doi.org/10.1002/jmri.24787
62. Yang, C.T., Chuang, K.H.: Gd(iii) chelates for MRI contrast agents: from high relaxivity to "smart", from blood pool to blood–brain barrier permeable. Med. Chem. Commun. **3**, 552–565 (2012). https://doi.org/10.1039/C2MD00279Ehttps://doi.org/10.1039/C2MD00279E
63. Kang, S.I., Ranganathan, R.S., Emswiler, J.E., et al.: Synthesis, characterization, and crystal structure of the gadolinium(III) chelate of (1R,4R,7R)-.alpha., alpha′., alpha″.-trimethyl-1,4,7,10-tetraazacyclododecane-1,4,7-triacetic acid (DO3MA). Inorg. Chem. **32**, 2912–2918 (1993). https://doi.org/10.1021/ic00065a019https://doi.org/10.1021/ic00065a019
64. Chang, C.A., Francesconi, L.C., Malley, M.F., et al.: Synthesis, characterization, and crystal structures of M(DO3A) (M = iron, gadolinium) and Na[M(DOTA)] (M = Fe, yttrium, Gd). Inorg. Chem. **32**, 3501–3508 (1993). https://doi.org/10.1021/ic00068a020https://doi.org/10.1021/ic00068a020
65. Aime, S., Botta, M., Fasano, M., Terreno, E.: Lanthanide(III) chelates for NMR biomedical applications. Chem. Soc. Rev. **27**, 19–29 (1998). https://doi.org/10.1039/A827019Zhttps://doi.org/10.1039/A827019Z
66. Caravan, P.: Strategies for increasing the sensitivity of gadolinium based MRI contrast agents. Chem. Soc. Rev. **35**, 512–523 (2006). https://doi.org/10.1039/B510982Phttps://doi.org/10.1039/B510982P
67. Aime, S., Barge, A., Batsanov, A.S. et al.: Controlling the variation of axial water exchange rates in macrocyclic lanthanide(iii) complexes. Chem. Commun. 1120–1121 (2002). https://doi.org/10.1039/B202862J
68. Thompson, A.L., Parker, D., Fulton, D.A., et al.: On the role of the counter-ion in defining water structure and dynamics: order, structure and dynamics in hydrophilic and hydrophobic gadolinium salt complexes. Dalt. Trans. 5605–5616 (2006). https://doi.org/10.1039/B606206G
69. Caravan, P., Farrar, C.T., Frullano, L., Uppal, R.: Influence of molecular parameters and increasing magnetic field strength on relaxivity of gadolinium- and manganese-based T1 contrast agents. Contrast Media Mol. Imaging **4**, 89–100 (2009). https://doi.org/10.1002/cmmi.267https://doi.org/10.1002/cmmi.267
70. Ibrahim, M.A., Hazhirkarzar, B., Dublin, A.B.: Magnetic Resonance imaging (MRI) gadolinium. In: StatPearls Publ. Treasure Isl. https://www.ncbi.nlm.nih.gov/books/NBK482487/. Accessed 5 May 2020
71. Magnevist® (gadopentetate dimeglumine) injection 0.5 mmol/mL. https://www.radiologysolutions.bayer.com/sites/g/files/kmftyc641/files/MVEOSLetter-GPOPDFR8v1.pdf. Accessed 8 July 2020
72. Gadolinium-Containing Contrast Agents. https://www.ema.europa.eu/en/medicines/human/referrals/gadolinium-containing-contrast-agents. Accessed 8 July 2020
73. Li, D., Larson, A.C., Speck, O., et al.: Modern applications of MRI in medical sciences. Magn. Med. 343–476 (2006)
74. Caravan, P.: Protein-targeted gadolinium-based magnetic resonance imaging (MRI) contrast agents: design and mechanism of action. Acc. Chem. Res. **42**, 851–862 (2009). https://doi.org/10.1021/ar800220phttps://doi.org/10.1021/ar800220p
75. Laurent, S., Vander, E.L., Muller, R.N.: Comparative study of the physicochemical properties of six clinical low molecular weight gadolinium contrast agents. Contrast Media Mol. Imaging **1**, 128–137 (2006). https://doi.org/10.1002/cmmi.100https://doi.org/10.1002/cmmi.100

76. Prince, M.R., Zhang, H., Zou, Z., et al.: Incidence of immediate gadolinium contrast media reactions. Am. J. Roentgenol. **196**, W138–W143 (2011). https://doi.org/10.2214/AJR.10.4885https://doi.org/10.2214/AJR.10.4885
77. Grobner, T.: Gadolinium—a specific trigger for the development of nephrogenic fibrosing dermopathy and nephrogenic systemic fibrosis? Nephrol. Dial. Transplant. **21**, 1104–1108 (2006). https://doi.org/10.1093/ndt/gfk062https://doi.org/10.1093/ndt/gfk062
78. Idée, J.-M., Port, M., Medina, C., et al.: Possible involvement of gadolinium chelates in the pathophysiology of nephrogenic systemic fibrosis: a critical review. Toxicology **248**, 77–88 (2008). https://doi.org/10.1016/j.tox.2008.03.012
79. Kanda, T., Fukusato, T., Matsuda, M., et al.: Gadolinium-based contrast agent accumulates in the brain even in subjects without severe renal dysfunction: evaluation of autopsy brain specimens with inductively coupled plasma mass spectroscopy. Radiology **276**, 228–232 (2015). https://doi.org/10.1148/radiol.2015142690https://doi.org/10.1148/radiol.2015142690
80. Thomsen, H.S., Morcos, S.K., Almén, T., et al.: Nephrogenic systemic fibrosis and gadolinium-based contrast media: updated ESUR Contrast Medium Safety Committee guidelines. Eur. Radiol. **23**, 307–318 (2013). https://doi.org/10.1007/s00330-012-2597-9https://doi.org/10.1007/s00330-012-2597-9
81. Brücher, E., Tircsó, G., Baranyai, Z., et al.: Stability and toxicity of contrast agents. In: The Chemistry of Contrast Agents in Medical Magnetic Resonance Imaging, pp. 157–208. John Wiley & Sons Ltd., Chichester (2013)